

CNRS
Centre National de la Recherche Scientifique

INFN
Istituto Nazionale di Fisica Nucleare



VSR1 cavity finesse measurements

F. Marion, B. Mours, L. Rolland, E. Tournefier

LAPP-Annecy

VIR-052A-08

June 19, 2008

VIRGO * A joint CNRS-INFN Project
Project office: Traversa H di via Macerata - I-56021 S. Stefano a Macerata, Cascina (PI)
Secretariat: Telephone (39) 50 752 521 – Fax (39) 50 752 550 – e-mail virgo@pisa.infn.it

Contents

1	Introduction	2
2	Finesse reconstruction method	3
2.1	Estimation of the cavity length as function of time	3
2.2	Simulation of the Airy peak shapes	5
2.3	Fit of the Airy peaks	6
3	Measurements of the cavity finesse during VSR1	7
3.1	Measurements from Airy peaks in free swinging cavities	7
3.2	Comparison with the locked cavity power variations	7
4	Conclusion	15
A	SIESTA configuration file	17
B	Measurements during VSR1	18

1 Introduction

The long cavities of the Virgo interferometer (north and west arms) consist in Fabry-Perot cavities when the interferometer is locked to take data in Science Mode. They are used to increase the power of the laser that is stored in the cavities.

The response of Virgo to a change in the cavity differential length is a modification of the laser power measured at the level of the dark fringe. It is defined as a transfer function in W/m.

When a cavity is locked, its response to a length modification behaves as a simple pole whose frequency depends on the finesse of the cavity. The average response of the cavities is taken into account in the reconstruction of the strain signal $h(t)$ to search for gravitational waves. The finesses of the cavities are expected to vary by a few percent as function of the mirror temperatures [1, 2].

The aim of this note is to estimate the variations of the finesses during the run VSR1 (May 18th to October 1st, 2007).

The method used to determine the cavity finesse, based on the comparison of the Airy peaks in the data with simulations, is described in the first section. The results and monitoring of the cavity finesse during VSR1 are then given. They are then compared to the variation of the power transmitted by the cavities.

2 Finesse reconstruction method

The finesse of the Fabry-Perot cavities depends on the mirror amplitude reflectivities ρ_1 and ρ_2 as:

$$F = \frac{\pi\sqrt{R}}{1-R} \quad (1)$$

$$\text{with } R = \rho_1\rho_2 \quad (2)$$

The intensity reflection coefficients are defined as $r_1 = \rho_1^2$ and $r_2 = \rho_2^2$.

It can also be extracted from the TEM₀₀ (Transverse Electro-Magnetic) Airy peaks [3]. Airy peaks are visible in the time variation of the power stored in the cavity when the length of the cavity changes. The powers in the north and west cavities are monitored through photodiodes in the external end-benches. The channel names are Pr_B7_DC and Pr_B8_DC respectively.

The finesse is defined as the ratio of the distance between two consecutive TEM₀₀ resonances (FSR, Free Spectral Range) to their linewidth (FWHM, Full Width Half Maximum). However, due dynamical effects, the Airy peaks are distorted and the line width cannot be measured directly. The distortion depends on the speed of the cavity mirrors. This parameter can be set in a dynamical simulation of a cavity which predicts the shape of the Airy peaks. A fit of the data with the simulation allows to estimate the finesse.

2.1 Estimation of the cavity length as function of time

The speed of the cavity is estimated from the cavity length time variation. The variation of the cavity length between two TEM₀₀ resonances is equal to $\lambda/2$ where λ is the wavelength of the laser (1064 nm).

An exemple of the cavity power as function of time is given in the figure 1. In order to reconstruct the cavity length time variations, the issue is to find the cavity length extrema. A few parameters have been defined from three Airy peaks ($i-1$) to ($i+1$) around the current one indexed by i : the amplitudes and widths of the peaks, A_j and W_j , and the time between the peaks: $\Delta t_j = t_j - t_{j-1}$. The following conditions are used to define an extremum:

- when the Airy peak is at one extremum (speed close to 0), it is much larger than its neighbours: $W_i > 2W_{i-1}$ and $W_i > 2W_{i+1}$.
- when the Airy peak is after the length extremum and the extremum is close to next peak: $\Delta t_i > \Delta t_{i-1}$ and $\Delta t_i > \Delta t_{i+1}$ and $W_i > 1.05W_{i+1}$
- when the Airy peak is soon after the length extremum: $\Delta t_i < \Delta t_{i-1}$ and $\Delta t_i < \Delta t_{i+1}$ and $W_i > 1.05W_{i+1}$

If these conditions are not fulfilled, the cavity length is incremented by $\pm\lambda/2$ depending on the current direction. An exemple of reconstructed cavity length time variation is shown in the figure 1.

If the cavity is excited but not too much (angularly and longitudinally), its length varies sinusoidally with time. A cosine function can be fit to the points: $l(t) = a_i + b_i \cos(\omega_i t + \Phi_i)$. For a given Airy peak at t_i , the fit is computed over a window of ?? s (or extended in order to enclose at least 5 peaks). The speed is then derived from $l(t)$ as $|v(t_i)| = b_i \omega_i \sin \omega_i t_i + \Phi_i$.

The cavity length can be reconstructed in different types of data.

- free swinging cavity: the cavity length variation is not really sinusoidal. The determination of its extrema, and therefore the cavity speed are not precise.
- swinging cavity with one mirror excited with a ~ 1 Hz line. The cavity length variation is dominated by the 1 Hz excitation and the speed is reconstructed within $\sim 20\%$.

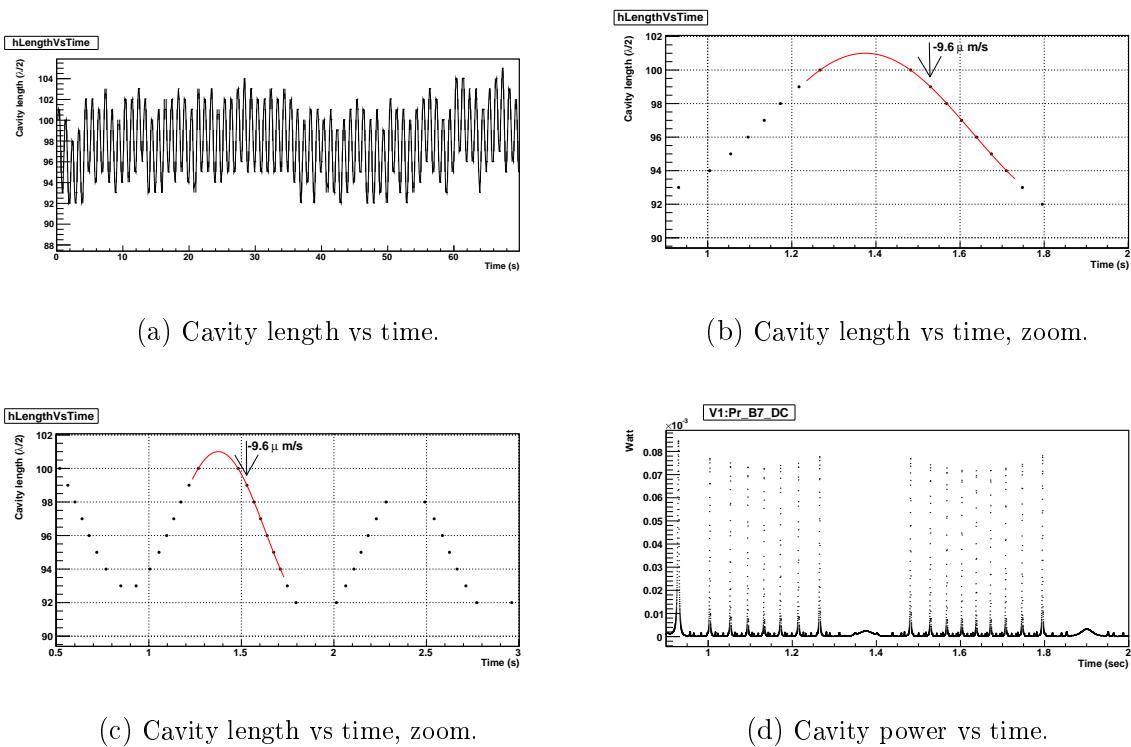


Figure 1: Cavity power and estimated length vs time. (a) Reconstructed north cavity length variations for a dataset with specific injections. (b) Reconstructed cavity length variations in a short window, with the cosine fit. (c) Same, but with larger time window. (d) NE cavity power (Pr_B7_DC) as function of time in the same window as (b).

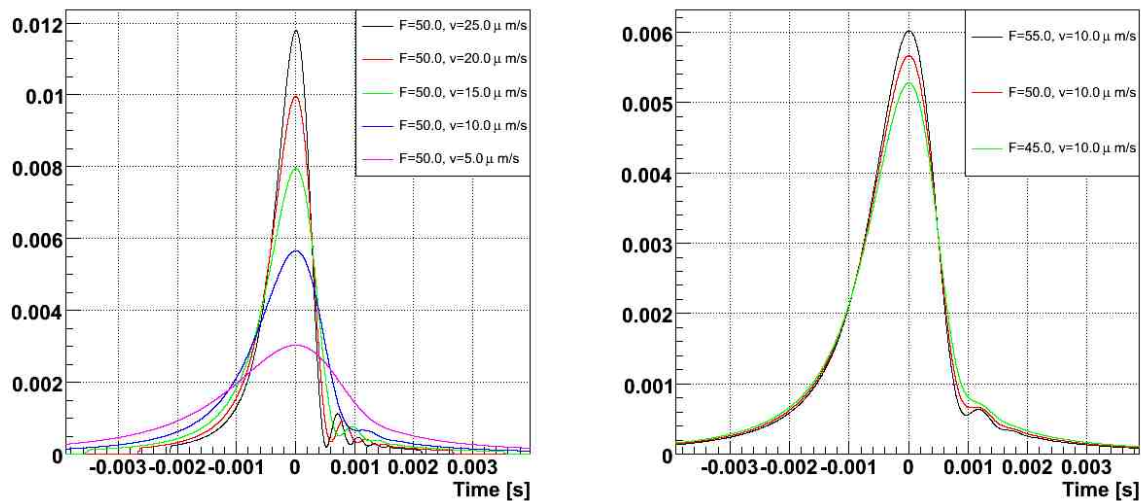
2.2 Simulation of the Airy peak shapes

The time domain simulation of a Fabry-Perot cavity including dynamical effects is computed using the SIESTA¹ program [4].

A set of simulations are performed scanning the cavity speed and finesse from 0.5 to $30\mu\text{m/s}$ and 40 to 60 respectively, with steps of 1 for both parameters. The time serie of the simulated photodiode readout is sampled at 20kHz .

Typical values of the mirror reflectivities (in intensity) are initially set to $r_1 = 0.882$ and $r_2 = 0.999957$. For a given cavity finesse, the reflection r_1 of the input mirror of the cavity is modified accordingly to equation 2 in the simulation. The speed of the cavity elongation is directly a parameter of the simulation configuration. An exemple of SIESTA configuration file is given in annexe.

For every sets of parameters (speed, finesse), the time serie of the simulated Airy peak is stored in a 3-dimension table within ± 0.020 ms (801 samples) around the peak maximum. The amplitude of the peak is set such that the integral of the time serie is 1. The shape of the Airy peaks is then linearly interpolated between the different simulated sets in order to have a continuous function. The figure 2 shows the shape of the Airy peaks as function of the cavity finesse for a speed of $10\mu\text{m/s}$ and as function of the cavity speed for a finesse of 50 .



(a) Finesse 50.

(b) Speed $10\mu\text{m/s}$

Figure 2: *Shape of the simulated Airy peaks (a) as function of the cavity speed for a finesse of 50. (b) as function of the cavity finesse for a speed of $10\mu\text{m/s}$,*

¹SIESTA version v4r00

2.3 Fit of the Airy peaks

Errors of $\pm 10^{-7}$ W have been used for the measurements of the cavity power time series Pr_B7,8_DC ($\pm 1.7 \cdot 10^{-3}$ V for the voltage time series Pr_B7,8_d1,2_DC). Every Airy peak i detected in this time serie is fitted using MIGRAD². The fit has four parameters: time of the maximum, amplitude, cavity finesse and cavity speed (when using the voltage channels Pr_B7,8_d1,2_DC (in V), an offset is added as a fifth parameter).

The initial time of the peak is set to its maximum t_i . This parameter is constrained within $\pm 200 \mu\text{s}$ around t_i . The initial amplitude is set to the integral of the measured Airy peak. The initial value of the finesse is set to its nominal value of 50. The initial speed of the cavity is set to the estimation described above. When the cavity length is close to a sine (with the 1 Hz excitation), the speed is constrained to vary by less than 30% from its initial value. Else, it is let free.

The Airy peaks with an estimated cavity speed outside the range $[3; 20] \mu\text{m/s}$ are not used. A few cuts are applied in order to select the “good quality” fits.

- no error returned by MIGRAD,
- the parameters are not close to the edge of the simulated table,
- χ^2 probability higher than 10%.

²GRADient MInimisation

3 Measurements of the cavity finesse during VSR1

3.1 Measurements from Airy peaks in free swinging cavities

No specific data were taken during VSR1 to measure the finesse of the cavities. Datasets with free swinging mirrors have been selected. The criteria were at least 30 seconds (and maximum 500 seconds) of data in step 0, with the BS and cavity mirrors aligned (i.e. $Sc_NE_Gain_tyMarMis = 0$) and PR misaligned ($Sc_PR_Gain_tyMarMis = -150$).

About 600 datasets have been selected during VSR1. The north and west cavity finesse have been fit using the voltage signal $Pr_B7_d1_ACp$ and power signal Pr_B8_DC respectively. Since the cavities are not excited, the cavity motion is not well estimated. Thus the speed is let free in the Airy peak fits.

For every datasets, some checks are performed on a few distributions. Examples are shown in the figures 3, 4, 5 and 6. The mean of the distribution of the error-weighted fitted finesse is a way to measure the finesse of the dataset. The fitted finesse as function of the fitted speed (before the selection on the speed) is used to check that there is no correlation between both parameters. The relative difference between the fitted speed and its initial estimation is not really usefull since the initial estimation is rather bad. The difference between the fitted time of the maximum and its initial value is lower than $100 \mu s$.

The datasets are then selected using a few quality criteria. The number of correctly fitted Airy peaks must be higher than 100. Four estimations of the finesse are performed: the average values of the raw and error-weighted finesse distributions, the value from a Gaussian fit of the raw distribution and the median value of the fitted finesse. The differences between the values must be lower than 0.5. The error of the Gaussian fit and the fitted sigma of the distribution must be lower than 0.5 and 1 respectively.

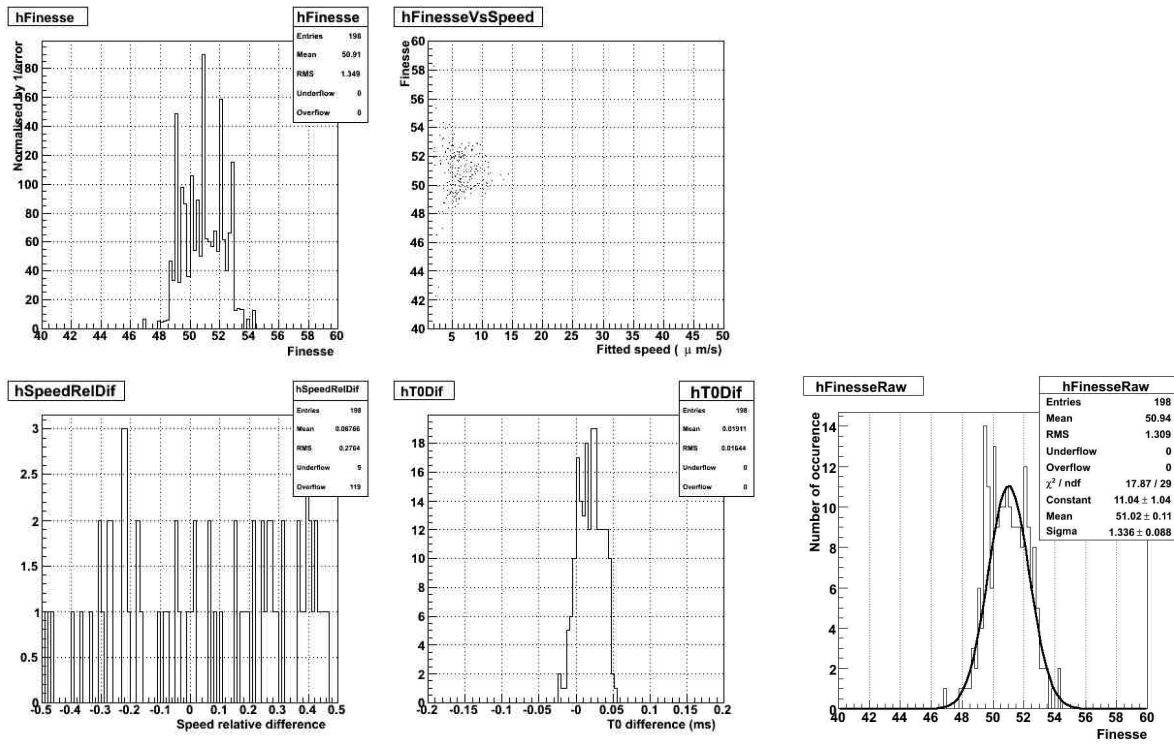
For the datasets passing the quality criteria, the finesse obtained from the Gaussian fit are given in appendix B and shown in the figure 7. Time variations are clearly visible, with amplitude of ± 1.5 around the average value for both cavities. The average values obtain from the few measurements during VSR1 are 49.1 and 51.5 for the north and west cavities respectively.

3.2 Comparison with the locked cavity power variations

When the interferometer is locked (step 12), the north and west cavities are controlled such that the laser TEM00 mode resonates. The mirror relative positions are thus controlled such that the power that is stored inside the cavity is at a maximum of an Airy peak.

The power stored in the cavity, measured through the channels $Pr_B\{7,8\}_DC$, is proportionnal to the cavity finesse. The relative variation of the cavity power gives a measurement of the relative variation of the cavity finesse.

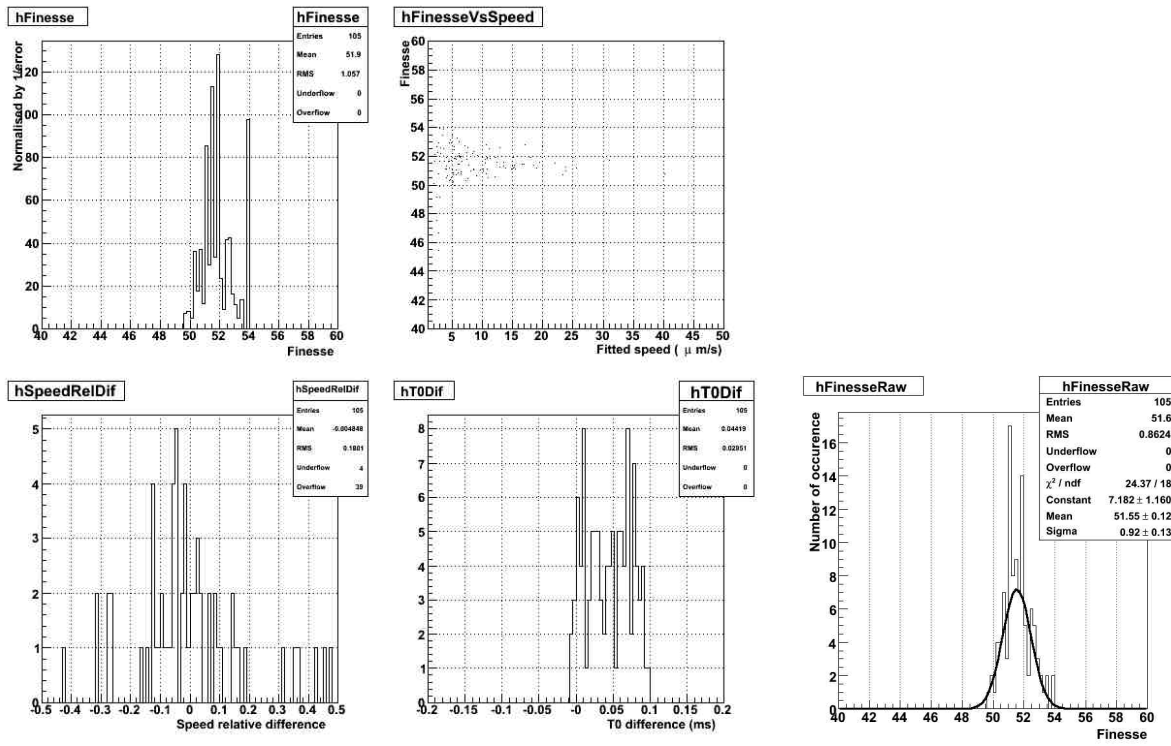
The variations of the cavity powers in step 12 during VSR1 have been computed. They



(a) Checks

(b) Raw fitted finesse

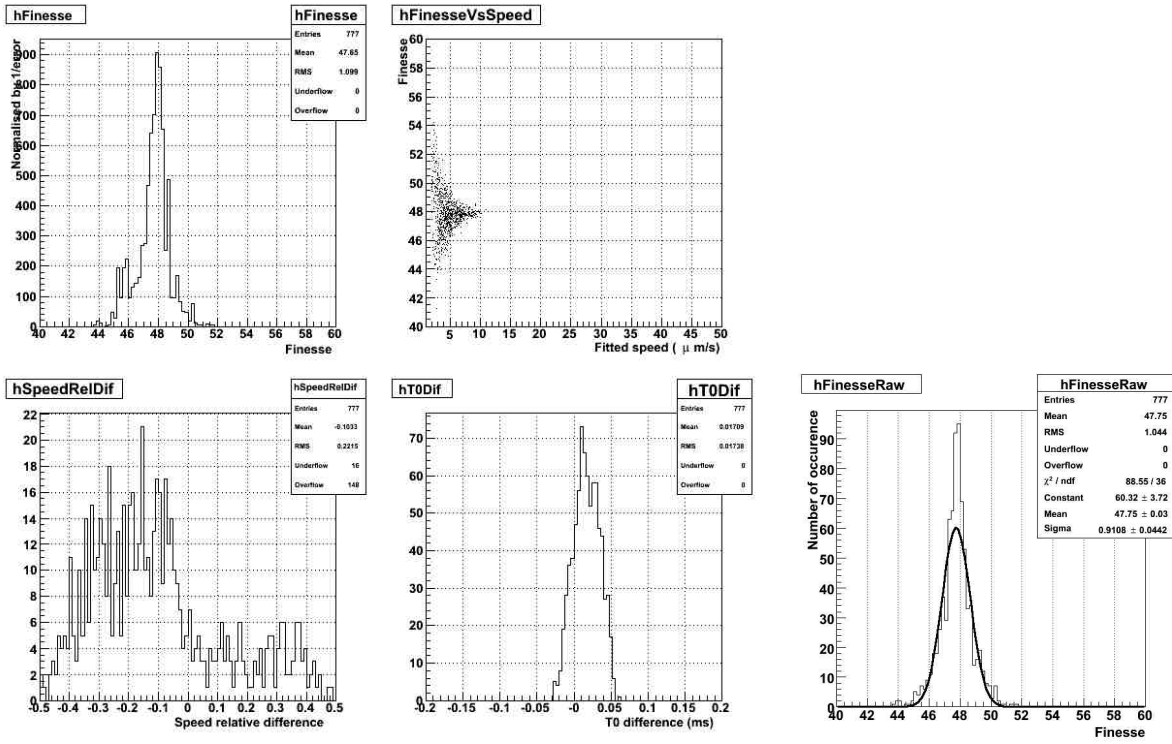
Figure 3: *Distributions for the north cavity at GPS 865551091. (a) Distribution of the error-weighted fitted finesse, finesse as function of speed, relative speed difference, time difference. (b) Distribution of the fitted finesse.*



(a) Checks

(b) Raw fitted finesse

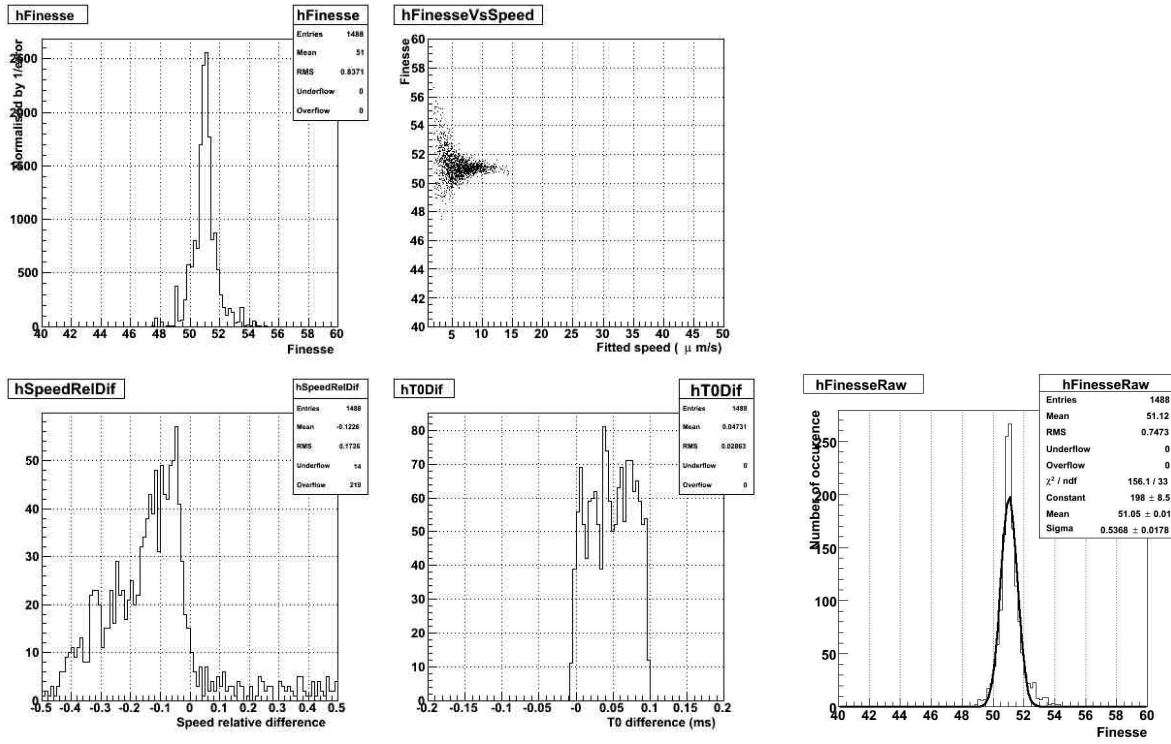
Figure 4: *Distributions for the west cavity at GPS 865551091. (a) Distribution of the error-weighted fitted finesse, finesse as function of speed, relative speed difference, time difference. (b) Distribution of the fitted finesse.*



(a) Checks

(b) Weighted finesse

Figure 5: *Distributions for the north cavity at GPS 868086730. (a) Distribution of the fitted finesse, finesse as function of speed, relative speed difference, time difference. (b) Distribution of the error-weighted fitted finesse.*



(a) Checks

(b) Weighted finesse

Figure 6: *Distributions for the west cavity at GPS 868086730. (a) Distribution of the fitted finesse, finesse as function of speed, relative speed difference, time difference. (b) Distribution of the error-weighted fitted finesse.*

have been normalised such that they match, on average, the finesse where there are direct measurements within one hour (normalisation factors of 575 and 627 for the north and west cavity powers respectively). The comparison of the finesse variations estimated by both methods are shown in the figure 8. A zoom on the beginning of the run (figure 9), when the etalon effect changed by one period on the NI mirror due to temperature variations.

The behavior of the cavity finesse measured in this note and the transmitted power of the cavities are similar. It somehow validate the measurements using the Airy peak shape. However, two types of systematic errors can be highlighted:

- during periods with constant transmitted power value, the dispersion of the cavity finesse measurements is of the order of 0.2,
- the normalisation factor of the cavity power might change as function of time. It is expected to change due to different mirror and/or photodiode alignments. Using a constant normalisation factor during VSR1, differences up to 1 are seen between the normalized power and the finesse.

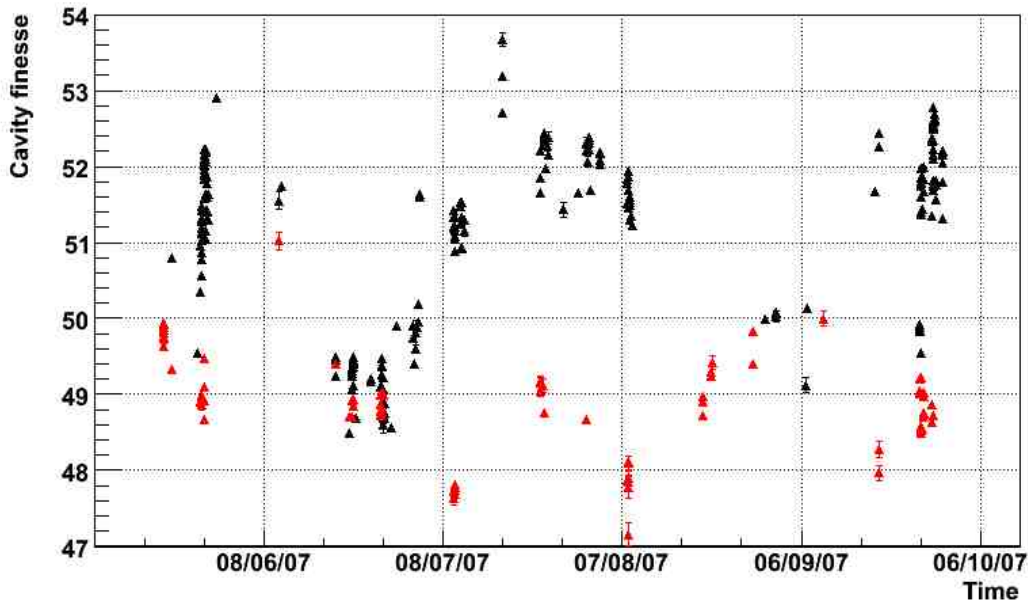


Figure 7: *Finesse vs time during VSR1 for the west (black) and north (red) cavities. The lines gives the average values during the run.*

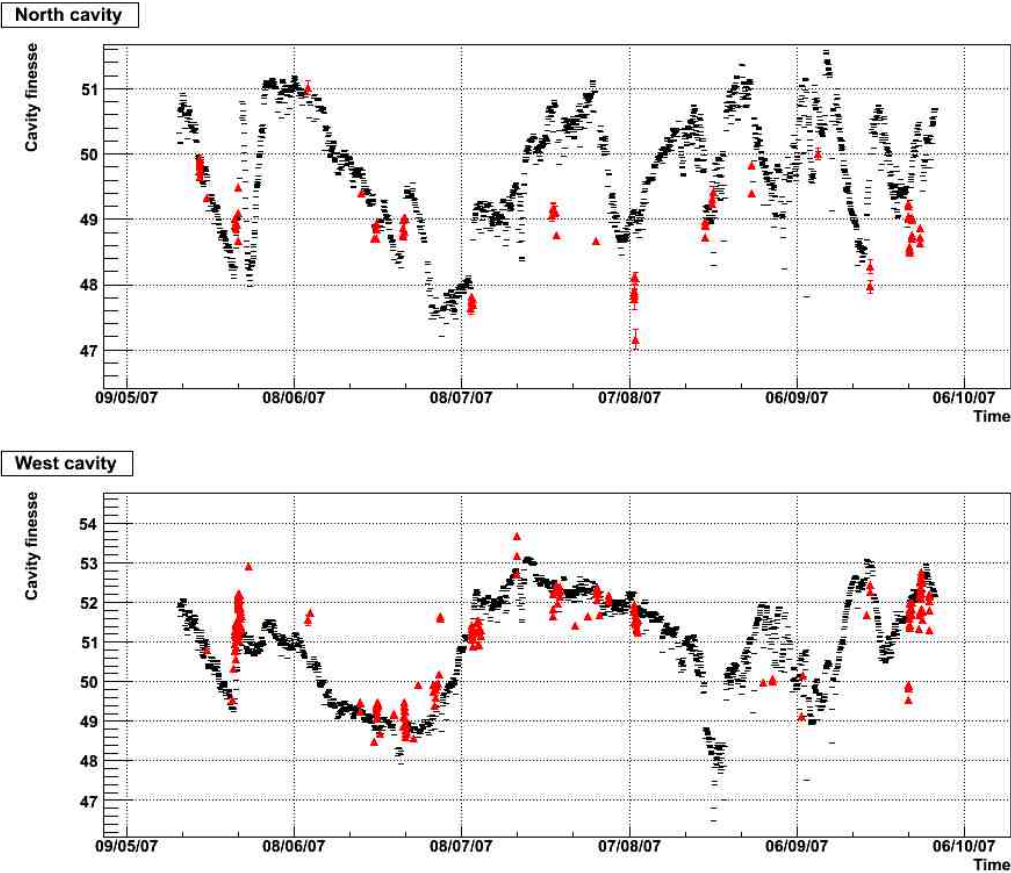


Figure 8: Cavity finesse and normalised power transmitted by the north and west cavities. The transmitted powers have been normalised by 575 and 627 respectively.

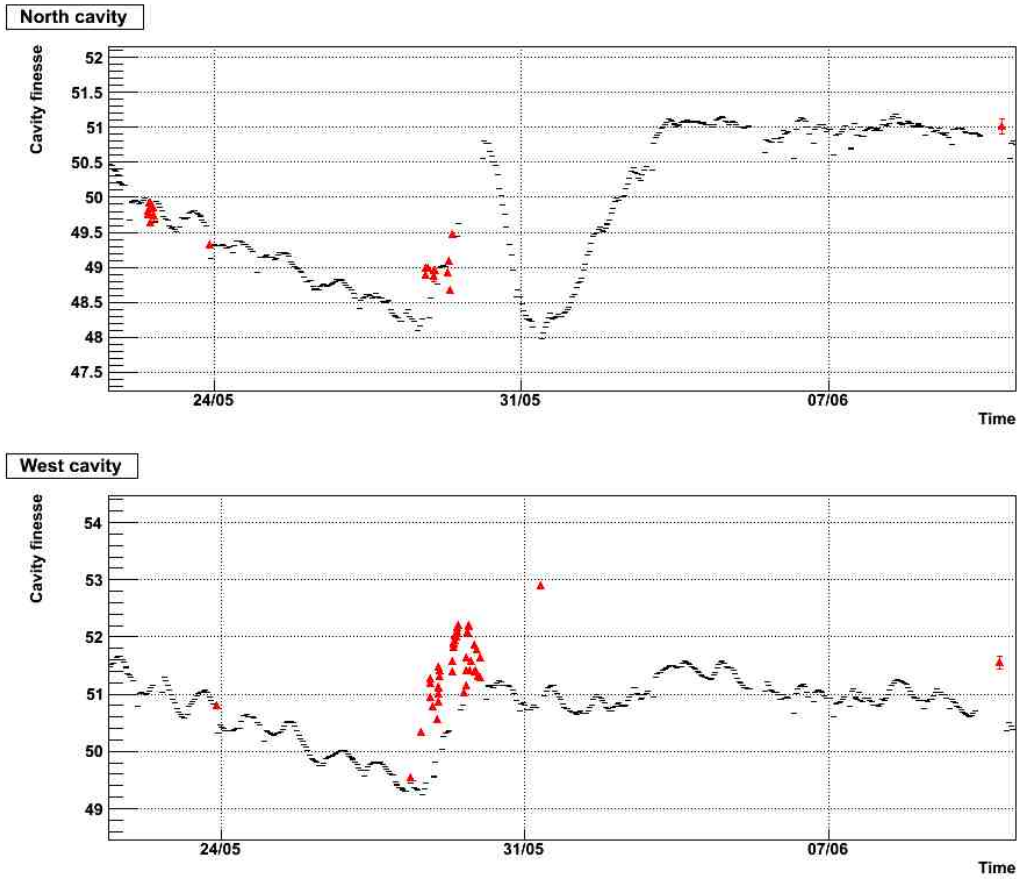


Figure 9: Zoom on the cavity finesse and normalised power transmitted by the north and west cavities. During this period, the etalon effect of the NI mirror went along a full period due to high temperature variations.

4 Conclusion

The finesse of the north and west cavities have been measured during VSR1 using the shape of the Airy peaks seen in the transmitted power of the free swinging cavities. It permits to monitor the absolute value of the finesse and to estimate the amplitude of the finesse variation to about ± 2 around their average values, as expected from the etalon effect in the input mirrors. Systematic errors of the order of 0.2 can be estimated from the dispersion of the measurements within short time-scales.

The variations of the measured finesse follow the variations of the power transmitted by the locked cavities. Differences of the order of 2% ($\Delta F \sim 1$) can be used as pessimistic systematic errors on the absolute value of the finesse using the Airy peak shape.

References

- [1] M. Punturo, *The mirror resonant modes method for measuring the optical absorption* (2007) VIR-001A-07
- [2] M. Punturo, *Etalon effect in the Virgo cavities*, slides of weekly meeting from June 12th 2007
- [3] F. Acernese et al. (Virgo collaboration) **Applied Optics** **46**, Issue 17, pp 3466-3484 (2007). *Measurements of the optical parameters of the VIRGO interferometer.*
- [4] B. Caron et al. **Astroparticle Physics** **10**, 369-386 (1999). *SIESTA, a time domain, general purpose simulation program for the VIRGO experiment.*

A SIESTA configuration file

Configuration file for the SIESTA simulation. In this simulation, the NE mirror is moving at $10 \mu\text{m/S}$ (MISweep). The NE and NI reflection coefficients are respectively 0.999957 and 0.881968. The simulated finesse is thus 50.

```

/* Creation of the clocks for signal simulation (rates) */
/* UJclock name          totalTime nClocks Freq0 Freq1 */
UJclock  masterClocks  80000    2      80000  1

/* Creation of the frame builder to store the output signals into a frame file */
UFrBuilder FBuilder 1 1 0 0

/* ***** Creation of the mirrors with their surface ***** */

/* *** NI,back *****/
/*Mirror name          clock susPos thermPos frontSurf backSurf initPos   initOrientation */
Mirror  Mir11          0      NULL  NULL    NULL      MiSu11b  6.4 0. 0.  1. 0. 0.
/* MIsurf name          curvature radius thetaX thetaY halfThickness reflection losses */
MIsurf  MiSu11b        0.      .2    0.     0.     0.      0.881968  .1e-3

/* *** NE, front *****/
Mirror  Mir12          0  NULL  NULL  MiSu12f  NULL  3006.4 0. 0.  1 0. 0.
MIsurf  MiSu12f        2.81294e-4 .2  0.  0.  0.  0.999957  0.

/* *** WI, back *****/
Mirror  Mir21          0  NULL  NULL  NULL  MiSu21b  0. 5.6 0.  0. 1. 0.
/*MIsurf  MiSu21b        0. .2 0.  0.  0.  0 .1e-3 */
MIsurf  MiSu21b        0. .2 0.  0.  0.  0  0

/* *** WE, front *****/
Mirror  Mir22          0  NULL  NULL  MiSu22f  NULL  0. 3005.6 0.  0. 1. 0.
MIsurf  MiSu22f        2.89855e-4 .2  0.  0.  0.  0  0.

/* *** BS, front *****/
Mirror  Mirbs          0  NULL  NULL  MiSubsf  NULL  0. 0. 0.  1. -1. 0.
MIsurf  MiSubsf        0. .2 0.  0.  0.  .5  0.

/* *** PR, front *****/
Mirror  Mirrc          0  NULL  NULL  NULL  MiSurcf  -6. 0. 0.  1. 0. 0.
MIsurf  MiSurcf        0. .2 0.  0.  0.  0.  0.

```

```

/* Define a mirror movement */
/* MISweep name  clock mirror startPos slope(m/s) axis (0=x, 2=z) */
MISweep  sweepz 0      Mir12  0.      1e-05  2

/* Create the laser */
/*IOLaser name  clock surf wavelength power noise noise curvature waist window method */
IOLaser  laser 0      NULL 1.064e-6  .56  NULL  NULL  0.      .021 .40  NO  0
/* Create the phase modulator */
OPmod  mod 0  laser.oBeam 3  0. 6.26408e6 -6.26408e6 carrier NULL sb1 NULL sb2 NULL
/* Create the signals for amplitude modulation of the side bands */
USignal carrier 0.99
USignal sb1      0.075
USignal sb2      -0.075

/*dynamic simulation*/
OPglobal itf 0 mod.oBeam MiSubsf  MiSu11b  MiSu12f MiSu21b  MiSu22f  MiSurcf NO NULL

/* Create the photodiodes */
/*OPdiode name clock efficiency demodFreq  demod incidentBeam  withShotNoise? */
OPdiode  B1  0  1.      6.26408e6  NULL  itf.oBeam1  YES
OPdiode  B7  0  1.      6.26408e6  NULL  itf.oBeam7  YES
OPdiode  B5  0  1.      6.26408e6  NULL  itf.oBeam5  YES

/* Simulate local readout */
/*UFRdout clock adcname      input      gain ADCbits type */
UFRdout  0  Pr_B7_DC  B7.dc  1.  -32  adc
UFRdout  0  Pr_B1_DC  B1.dc  1.  -32  adc

/* Save output to the frame file */
/* UFRFile clock filename Ascii? frame framePerFile */
UFRFile -1 finesse_tmp NO FBuilder.frameH 1

```

B Measurements during VSR1

The measured finesse for all the selected datasets during VSR1 are given in the following tables for the west and the north cavities.

GPS	N_{peaks}	F_{fit}	F_{medium}	GPS	N_{peaks}	F_{fit}	F_{medium}
863992195.	110	50.800 ± 0.0550	50.780	864471314.	920	52.160 ± 0.0160	52.420
864376813.	121	49.550 ± 0.0600	49.170	864471824.	769	52.220 ± 0.0180	52.210
864398035.	170	50.340 ± 0.0380	50.810	864484745.	209	51.040 ± 0.0400	51.210
864416338.	1204	50.950 ± 0.0180	51.340	864487844.	264	51.150 ± 0.0460	51.560
864417332.	145	51.190 ± 0.0250	50.970	864489180.	1390	51.420 ± 0.0160	51.550
864417505.	108	51.280 ± 0.0480	51.210	864489690.	336	51.640 ± 0.0300	51.610
864421666.	206	50.780 ± 0.0300	50.870	864490760.	944	52.070 ± 0.0150	51.680
864432035.	252	50.560 ± 0.0410	50.270	864492290.	823	52.090 ± 0.0140	52.320
864432387.	477	50.870 ± 0.0180	51.010	864492800.	779	52.180 ± 0.0150	52.520
864432585.	503	51.020 ± 0.0180	51.190	864493310.	715	52.190 ± 0.0180	52.410
864432929.	346	51.130 ± 0.0220	50.820	864493820.	751	52.220 ± 0.0180	51.920
864433804.	127	51.120 ± 0.0320	51.090	864494330.	765	52.200 ± 0.0180	52.310
864434450.	175	51.470 ± 0.0340	51.510	864496199.	114	51.420 ± 0.0520	51.180
864434905.	488	51.310 ± 0.0200	51.130	864498649.	357	51.590 ± 0.0270	51.820
864435877.	461	51.420 ± 0.0200	51.520	864504648.	323	51.870 ± 0.0260	51.500
864460604.	1562	51.400 ± 0.0160	51.450	864506129.	196	51.400 ± 0.0450	51.330
864461114.	1429	51.580 ± 0.0150	51.400	864507534.	989	51.420 ± 0.0160	51.440
864462644.	1048	51.830 ± 0.0170	52.000	864509704.	160	51.780 ± 0.0340	51.440
864463664.	995	51.900 ± 0.0190	51.900	864513173.	487	51.320 ± 0.0280	51.120
864464174.	937	51.880 ± 0.0190	52.300	864515972.	227	51.300 ± 0.0330	51.440
864465194.	644	51.950 ± 0.0280	51.710	864516452.	107	51.640 ± 0.0620	51.880
864466724.	903	52.030 ± 0.0190	52.290	864636538.	256	52.900 ± 0.0390	53.290
864467234.	864	52.010 ± 0.0200	52.330	865551091.	105	51.550 ± 0.120	52.020
864467744.	1016	52.020 ± 0.0170	52.490	865585638.	146	51.750 ± 0.0400	51.480
864468254.	962	52.070 ± 0.0150	52.500	866360104.	1291	49.250 ± 0.0140	49.180
864468764.	1180	52.020 ± 0.0120	52.230	866361124.	327	49.490 ± 0.0360	49.030
864469274.	1127	52.060 ± 0.0130	51.920	866364694.	127	49.450 ± 0.0640	49.780
864469784.	1026	52.070 ± 0.0150	51.800	866563538.	276	48.490 ± 0.0580	48.170
864470294.	1187	52.060 ± 0.0120	52.030	866607238.	108	49.060 ± 0.0610	49.470
864470804.	948	52.100 ± 0.0150	51.880	866607748.	166	49.250 ± 0.0460	49.030

Table 1: **West finesse measurements during VSR1.** For every datasets and every cavity, the number of correctly fitted Airy peaks is given (N_{peaks}). The finesse fitted on the raw finesse distribution and the medium value of the measured finesse are given.

GPS	N_{peaks}	F_{fit}	F_{median}	GPS	N_{peaks}	F_{fit}	F_{median}
866612136.	102	49.340 ± 0.0580	49.170	867052171.	1225	48.780 ± 0.0210	48.560
866612459.	629	49.320 ± 0.0210	49.590	867052681.	1029	49.060 ± 0.0190	48.840
866612969.	760	49.320 ± 0.0170	49.220	867053191.	664	49.230 ± 0.0240	49.530
866613479.	661	49.280 ± 0.0200	49.040	867061631.	100	48.590 ± 0.0920	48.870
866613989.	191	49.280 ± 0.0330	49.120	867061750.	160	48.690 ± 0.0750	48.580
866614591.	572	49.370 ± 0.0230	49.370	867066204.	335	48.680 ± 0.0400	48.950
866615977.	272	49.410 ± 0.0350	49.380	867066540.	114	48.880 ± 0.140	48.700
866618272.	586	49.420 ± 0.0220	49.520	867073484.	105	48.760 ± 0.0720	48.500
866618782.	599	49.430 ± 0.0220	49.330	867176122.	1183	48.560 ± 0.0130	48.950
866619486.	588	49.400 ± 0.0250	49.680	867258593.	115	49.910 ± 0.0480	49.830
866620412.	555	49.430 ± 0.0240	48.970	867488163.	181	49.750 ± 0.0550	49.510
866620922.	670	49.420 ± 0.0180	49.750	867496014.	181	49.910 ± 0.0480	50.080
866621432.	596	49.460 ± 0.0230	49.030	867503283.	192	49.400 ± 0.0560	49.710
866622653.	504	49.490 ± 0.0270	49.300	867517545.	112	49.810 ± 0.160	49.910
866624844.	628	49.490 ± 0.0220	49.470	867528953.	154	49.590 ± 0.0700	49.860
866632771.	941	49.120 ± 0.0260	48.670	867550048.	386	49.880 ± 0.0310	50.470
866661331.	442	48.680 ± 0.0470	48.760	867567000.	745	49.950 ± 0.0170	49.830
866873245.	111	49.170 ± 0.0420	49.100	867570608.	166	50.190 ± 0.0360	50.180
866873390.	128	49.200 ± 0.0500	49.710	867590498.	840	51.640 ± 0.0130	52.090
867020011.	328	49.100 ± 0.0250	49.520	867591518.	844	51.590 ± 0.0200	51.750
867028252.	1332	48.870 ± 0.0180	48.550	868073010.	639	51.180 ± 0.0240	51.190
867028762.	996	49.100 ± 0.0190	49.500	868074832.	610	51.200 ± 0.0230	51.640
867029944.	130	49.470 ± 0.0580	49.710	868076645.	211	51.180 ± 0.0370	50.960
867037697.	764	49.260 ± 0.0180	49.210	868076992.	1026	51.330 ± 0.0190	51.520
867038717.	609	49.370 ± 0.0180	49.900	868083060.	268	51.420 ± 0.0330	51.300
867039553.	362	49.470 ± 0.0290	49.690	868086730.	1488	51.050 ± 0.0150	50.970
867040992.	100	49.390 ± 0.0410	49.300	868087240.	611	51.150 ± 0.0230	51.500
867041718.	101	49.390 ± 0.0400	49.820	868089068.	567	51.080 ± 0.0210	51.060
867042448.	252	49.480 ± 0.0290	49.400	868089449.	183	51.210 ± 0.0350	51.240

Table 2: WE finesse measurements during VSRI (continued).

GPS	N_{peaks}	F_{fit}	F_{median}	GPS	N_{peaks}	F_{fit}	F_{median}
868090703.	254	51.330 ± 0.0280	51.260	869408282.	278	51.970 ± 0.0660	52.330
868092324.	321	50.890 ± 0.0350	50.900	869438162.	132	52.280 ± 0.0750	52.290
868095928.	691	51.050 ± 0.0260	51.500	869443891.	313	52.150 ± 0.0270	51.810
868173540.	558	51.250 ± 0.0350	51.640	869445179.	154	52.380 ± 0.0770	52.810
868174560.	404	51.480 ± 0.0440	51.950	869671060.	112	51.430 ± 0.0960	51.750
868175070.	401	51.520 ± 0.0300	51.200	869883229.	395	51.660 ± 0.0450	52.020
868190880.	1725	50.920 ± 0.0110	51.010	869999758.	241	52.210 ± 0.0350	52.280
868191390.	1841	50.940 ± 0.0110	50.630	870001288.	137	52.290 ± 0.0530	52.170
868191900.	403	51.530 ± 0.0410	51.170	870001798.	231	52.310 ± 0.0620	52.700
868192920.	372	51.330 ± 0.0340	51.270	870002818.	104	52.290 ± 0.0900	52.050
8682224898.	141	51.160 ± 0.0760	51.510	870022447.	102	52.060 ± 0.0760	52.330
8682226489.	239	51.300 ± 0.0280	50.900	870024575.	1182	52.300 ± 0.0120	51.980
868779680.	405	52.700 ± 0.0500	52.960	870027635.	489	52.340 ± 0.0300	51.830
868780190.	415	53.190 ± 0.0440	53.100	870028145.	175	52.380 ± 0.0590	52.060
868780700.	130	53.670 ± 0.0870	53.300	870028655.	312	52.320 ± 0.0390	52.030
869329199.	711	52.200 ± 0.0170	51.940	870029165.	139	52.220 ± 0.0680	52.720
869332419.	179	51.840 ± 0.0580	51.600	870060314.	549	51.680 ± 0.0380	52.030
8693333951.	312	51.660 ± 0.0380	51.500	870195691.	276	52.030 ± 0.0380	52.040
869382537.	351	52.380 ± 0.0430	52.500	870196337.	104	52.190 ± 0.0440	52.080
869383047.	472	52.340 ± 0.0240	52.030	870198992.	464	52.080 ± 0.0160	52.100
869383557.	429	52.420 ± 0.0310	52.470	870199365.	155	52.170 ± 0.0230	52.120
869384067.	642	52.370 ± 0.0190	52.410	870593932.	1112	51.510 ± 0.0280	51.900
869384577.	502	52.410 ± 0.0250	52.860	870594952.	1197	51.780 ± 0.0200	52.300
869388147.	562	52.430 ± 0.0190	52.740	870595462.	907	51.830 ± 0.0240	51.910
869388657.	481	52.410 ± 0.0360	52.900	870596482.	687	51.870 ± 0.0370	52.090
869389167.	970	52.320 ± 0.0160	52.020	870598522.	1001	51.940 ± 0.0350	51.720
869389677.	1199	52.290 ± 0.0130	52.300	870604132.	615	51.680 ± 0.0230	51.640
869391717.	497	52.320 ± 0.0390	52.770	870607715.	379	51.450 ± 0.0380	51.300
869392737.	1019	52.360 ± 0.0330	52.820	870608225.	350	51.460 ± 0.0580	51.580
869393247.	641	52.270 ± 0.0390	52.580	870628770.	445	51.300 ± 0.0310	51.280

Table 3: *WE* finesse measurements during VSR1 (continued).

GPS	N_{peaks}	F_{fit}	F_{median}	GPS	N_{peaks}	F_{fit}	F_{median}
870629238.	1628	51.490 ± 0.0120	51.740	874855437.	239	51.440 ± 0.0330	51.680
870629748.	361	51.530 ± 0.0300	51.450	874886065.	383	51.670 ± 0.0240	52.120
870631702.	892	51.570 ± 0.0140	52.070	874886253.	563	51.830 ± 0.0230	51.680
870633733.	249	51.590 ± 0.0300	51.680	874886661.	996	52.000 ± 0.0130	51.790
870638454.	222	51.350 ± 0.0320	51.360	875002463.	820	51.340 ± 0.0190	51.030
870657159.	772	51.230 ± 0.0210	51.010	875005523.	957	52.330 ± 0.0140	52.180
872590244.	208	49.990 ± 0.0530	49.480	875006033.	612	52.360 ± 0.0160	52.420
872734293.	493	50.070 ± 0.0200	50.100	875011555.	534	51.690 ± 0.0210	51.330
872735313.	261	50.070 ± 0.0420	50.340	875013558.	625	51.760 ± 0.0220	51.790
872735902.	167	50.080 ± 0.0600	50.520	875016509.	1021	51.750 ± 0.0130	51.940
872736412.	102	50.020 ± 0.0730	49.900	875017792.	326	52.230 ± 0.0230	52.350
873171637.	196	49.120 ± 0.100	48.610	875018528.	213	52.150 ± 0.0240	52.390
873202198.	454	50.140 ± 0.0490	50.160	875018686.	201	52.220 ± 0.0260	52.120
874178760.	826	51.670 ± 0.0170	51.960	875018803.	155	52.220 ± 0.0230	52.210
874235370.	275	52.260 ± 0.0600	52.060	875019983.	210	52.490 ± 0.0300	52.310
874236900.	166	52.440 ± 0.0480	52.590	875022121.	886	51.820 ± 0.0160	51.960
874828995.	589	49.830 ± 0.0160	50.000	875022631.	610	52.100 ± 0.0140	52.040
874829505.	1280	49.840 ± 0.0100	49.950	875023433.	604	52.230 ± 0.0100	52.660
874830015.	1016	49.890 ± 0.0110	50.140	875023720.	1810	52.350 ± 0.00562	52.390
874830525.	486	49.920 ± 0.0180	50.020	875024230.	763	52.510 ± 0.0120	52.770
874839195.	1167	49.550 ± 0.0120	49.580	875024740.	184	52.770 ± 0.0240	52.670
874843819.	185	51.370 ± 0.0350	51.800	875025250.	523	52.530 ± 0.0160	52.640
874849513.	582	51.410 ± 0.0180	51.820	875026270.	107	52.550 ± 0.0180	52.260
874849727.	133	51.600 ± 0.0390	51.450	875026604.	422	52.540 ± 0.0100	52.800
874849805.	425	51.740 ± 0.0240	51.850	875027014.	167	52.590 ± 0.0160	52.580
874849969.	187	51.780 ± 0.0210	51.780	875027740.	185	52.550 ± 0.0190	52.630
874851033.	276	51.790 ± 0.0240	51.690	875027889.	786	52.580 ± 0.00935	52.370
874851710.	229	51.840 ± 0.0150	51.820	875028869.	210	52.630 ± 0.0210	52.560
874852076.	110	51.970 ± 0.0330	51.890	875029477.	227	52.620 ± 0.0160	52.510
874852599.	130	51.840 ± 0.0450	51.730	875030407.	646	52.630 ± 0.0130	52.700

Table 4: *WE finesse measurements during VSRI (continued).*

GPS	N_{peaks}	F_{fit}	F_{median}
875030917.	478	52.590 ± 0.0120	52.580
875031347.	141	52.680 ± 0.0240	52.660
875032324.	221	52.600 ± 0.0220	53.130
875051411.	308	51.570 ± 0.0210	51.640
875053868.	803	51.810 ± 0.0160	51.870
875055480.	670	51.800 ± 0.0160	51.730
875057162.	556	51.760 ± 0.0200	51.770
875156646.	3027	51.310 ± 0.00615	51.340
875157156.	2349	51.800 ± 0.00535	51.910
875157666.	3148	52.040 ± 0.00372	52.300
875158686.	195	52.150 ± 0.0160	52.230
875158864.	757	52.190 ± 0.0100	51.930
875159390.	370	52.200 ± 0.0160	52.420

Table 5: *WE finesse measurements during VSR1 (continued).*

GPS	N_{peaks}	F_{fit}	F_{median}	GPS	N_{peaks}	F_{fit}	F_{median}
863870399.	768	49.810 ± 0.0100	49.910	867020011.	173	48.990 ± 0.0640	49.160
863870909.	355	49.760 ± 0.0210	50.060	867028252.	672	48.780 ± 0.0330	48.970
863871929.	364	49.930 ± 0.0470	49.820	867038207.	831	49.010 ± 0.0310	48.600
863872439.	562	49.920 ± 0.0180	49.670	867042119.	112	48.810 ± 0.120	49.160
863874479.	169	49.930 ± 0.0610	49.260	867042448.	393	49.030 ± 0.0480	48.960
863875499.	338	49.850 ± 0.0210	49.700	867052681.	518	49.010 ± 0.0420	49.100
863876009.	138	49.640 ± 0.0610	49.570	867053191.	337	49.000 ± 0.0560	48.930
863880599.	233	49.880 ± 0.0440	50.220	868066950.	234	47.640 ± 0.0900	47.460
863881109.	206	49.740 ± 0.0730	49.340	868080607.	608	47.730 ± 0.0400	47.960
863992195.	249	49.330 ± 0.0190	49.610	868086730.	777	47.750 ± 0.0350	47.770
864416338.	900	48.900 ± 0.0260	48.570	868087240.	376	47.810 ± 0.0470	48.380
864417332.	114	49.000 ± 0.0480	48.920	868090703.	270	47.770 ± 0.0510	47.590
864421666.	133	49.000 ± 0.0560	48.850	868097758.	367	47.690 ± 0.0460	47.920
864432035.	123	48.870 ± 0.0750	48.790	869322430.	135	49.050 ± 0.0770	48.690
864432929.	230	48.960 ± 0.0540	49.100	869332419.	104	49.150 ± 0.0800	49.510
864435877.	358	48.960 ± 0.0430	49.300	869333951.	188	49.170 ± 0.0780	49.490
864460094.	885	48.920 ± 0.0270	48.930	869378058.	256	49.120 ± 0.0870	49.290
864462134.	915	49.100 ± 0.0350	48.890	869386617.	985	48.760 ± 0.0310	49.190
864465704.	668	48.670 ± 0.0580	48.600	869997718.	238	48.670 ± 0.0550	48.850
864468764.	855	49.480 ± 0.0430	49.490	870595462.	496	47.860 ± 0.0480	47.380
865551091.	198	51.020 ± 0.110	50.760	870597502.	293	47.840 ± 0.0760	47.490
866369284.	574	49.400 ± 0.0200	49.330	870599542.	1268	48.120 ± 0.0150	48.090
866563538.	227	48.710 ± 0.0400	48.220	870602602.	177	47.910 ± 0.0960	47.320
866611178.	280	48.710 ± 0.0690	48.850	870603112.	128	47.780 ± 0.160	47.760
866612969.	462	48.920 ± 0.0530	49.400	870604132.	143	47.160 ± 0.150	47.030
866614591.	501	48.840 ± 0.0450	48.880	870605717.	129	48.090 ± 0.0910	48.220
866615101.	441	48.930 ± 0.0500	49.200	871686068.	842	48.720 ± 0.0330	48.710
867013500.	413	48.730 ± 0.0440	48.670	871687088.	1019	48.900 ± 0.0220	48.930
867016703.	249	48.780 ± 0.0670	48.980	871687598.	886	48.970 ± 0.0260	49.260
867018435.	634	48.860 ± 0.0380	48.360	871688108.	580	48.910 ± 0.0330	49.180

Table 6: **North cavity finesse measurements during VSR1.** For every datasets and every cavity, the number of correctly fitted Airy peaks is given (N_{peaks}). The finesse fitted on the raw finesse distribution and the median value of the measured finesse are given.

GPS	N_{peaks}	F_{fit}	F_{median}
871806059.	1028	49.300 ± 0.0150	49.270
871806569.	594	49.240 ± 0.0210	48.870
871812689.	153	49.420 ± 0.0890	49.470
872414255.	2269	49.400 ± 0.00570	49.270
872416805.	528	49.830 ± 0.0250	49.940
873425627.	230	50.000 ± 0.0960	49.860
874235370.	208	47.970 ± 0.0970	47.790
874236900.	179	48.280 ± 0.110	48.470
874828995.	820	49.040 ± 0.0310	49.430
874831545.	379	49.010 ± 0.0310	48.920
874832055.	133	49.200 ± 0.0660	49.150
874839195.	912	49.230 ± 0.0270	49.370
874849513.	405	48.580 ± 0.0210	48.610
874849805.	397	48.580 ± 0.0190	48.570
874849969.	199	48.530 ± 0.0270	48.700
874850492.	119	48.540 ± 0.0370	48.790
874851033.	219	48.490 ± 0.0230	48.590
874855437.	150	48.550 ± 0.0650	48.200
874884050.	2234	48.980 ± 0.00770	48.970
874886065.	146	48.700 ± 0.0530	49.120
874886253.	232	48.740 ± 0.0490	49.050
874886502.	280	49.020 ± 0.0270	48.620
874886661.	679	48.760 ± 0.0300	48.540
875006033.	381	48.630 ± 0.0440	48.420
875008084.	414	48.870 ± 0.0330	49.130
875013558.	296	48.720 ± 0.0530	48.880

Table 7: North cavity finesse measurements during VSR1 (continued).